SAND2019-8336C

Mechanical Behavior of Gold-Containing SAC396 Solder

R. Wheeling, S. Williams, T. Garcia, P. Vianco
Sandia National Laboratories, Albuquerque, New Mexico, USA
rwheeli@sandia.gov
505-845-7621

"Sandia National Laboratories is a multimission laboratory managed and operated by National Technology & Engineering Solutions of Sandia, LLC, a wholly owned subsidiary of Honeywell International Inc., for the U.S. Department of Energy's National Nuclear Security Administration under contract DE-NA0003525."

Abstract

Time independent (stress-strain) and time dependent (creep) deformation were investigated in gold (Au)-containing Sn-3.9Ag-0.6Cu (SAC 396) bulk solder alloys. Gold content was varied from 0-8 wt. % and three aging conditions were investigated at 5 test temperatures between -25 and 160 °C. The resulting mechanical behaviors of the alloys are discussed in this paper, and a discussion of fatigue properties will follow this work. Empirical parameters attained from the respective temperature dependent stress-strain curves, creep curves, and fatigue curves will be applied to a unified creep constitutive plasticity model (UCPM), to expand both low cycle and high cycle fatigue predictive capabilities, in a follow-on paper. Temperature appears to have the largest effect on yield stress, but in the industry's current solder joint operating temperatures, Au content has a much stronger influence on properties. Obtaining the mechanical test data for a range of Au-levels is the first step in incorporating reliable Au embrittlement trends into current low cycle fatigue (LCF) solder joint models and future high cycle fatigue (HCF) models, regarding electronic interconnect applications. This paper synthesizes the general mechanical behavior trends for a high level, qualitative overview.

Intro/Background

As the use of lead (Pb)-free solders increases, modeling capabilities must also expand. This work seeks to expand the predictive capacity of a viscoplastic damage model developed for lead-free solder in order elucidate gold (Au) embrittlement effects regarding low and high cycle fatigue behavior [1]. Thermal cycling and vibration conditions are generally associated with low and high cycle fatigue conditions, respectively. This study is divided into 4 portions:

1) a high level overview of mechanical behavior trends which accompany Au-content increases

2) applying the mechanical behavior data to current LCF models and developing an initial HCF predictive model from the experimental mechanical properties

3) validation study to compare the model with experimental, high cycle fatigue failures in solder joints of electronic assemblies

4) a more advanced modeling capability which couples the initial high cycle fatigue model with diffusion data to account for Au diffusion in solder joints.

This paper focuses on the first of the 4 areas.

Gold embrittlement, and the resulting mechanical property degradation, of solder joints has been well-studied in tin-lead (Sn-Pb) solder since the 1960s, yet the phenomenon remains relevant in the electronics industry since Au coatings are necessary in electronic assemblies [2-8]. Electronic assemblies contain Au layers to protect an adjacent substrate from oxidation and corrosion, enhance solder wetting, and/or improve wire bondability. Since Au readily dissolves into molten solder during soldering processes, various Au-Sn intermetallic compounds (IMCs) can form at interfaces and in bulk solder upon solidification; after solidification solid-state IMC growth can be supported throughout the lifetime of a solder joint [9-11].

Embrittled solder joints pose a serious risk to electronic system reliability, so understanding the necessary Au-levels to promote embrittled joints is key maintaining high reliability. Foster first reported lower elongation values coinciding with a transition from ductile to brittle fracture when 5-10 wt.% Au was present in 60-40 Sn-Pb solder [3]. Harding and Pressley simultaneously defined a critical Au plate thickness (1.25 micron) above which, measurable detrimental effects associated with embrittlement would be likely [12]. 3 wt. % Au in Sn-Pb solder joints is the generally accepted upper limit for embrittlement prevention in the electronics industry [2, 6, 9, 13-15].

While Au-embrittlement is recognized in Pb-free solders, the research body is limited, but the increased use of Pb-free solder warrants a comprehensive understanding regarding the effects of Au contamination on Pb-free solder microstructure and hence mechanical properties. As tin-silver-copper (Sn-Ag-Cu, “SAC”) alloys have emerged as strong contenders for Sn-Pb solder replacement in recent decades, this study addresses the Sn-3.9Ag-0.6Cu (SAC396) solder composition [10].

In SAC/Au systems diffusion layers of $AuSn_2$ and/or $AuSn_4$ form when Au dissolves into the liquid solder, and $AuSn_4$ precipitates during solidification [15-18]. Detailed metallographic and crystallographic analyses have also been published [15, 18, 19]. While recent investigations have attempted to determine Au-threshold limits, reports suggest that Au embrittlement in SAC solder alloys manifests through a longer-term progressive degradation with increasing Au content, relative to Sn-Pb solder alloys [6, 10]. When Au contents exceed 10 wt.%, solder joints perform poorly in mechanical tests, but below 5 wt. %, significant joint degradation is not realized. However, between 5 and 10 wt.%, interpretation is convoluted and a clear threshold limit is difficult to pinpoint [9]. Different behavior regarding the re-distribution of $AuSn_4$ precipitates has been reported between Pb-bearing and Pb-free solder upon aging [8]. Understanding the propensity for Au embrittlement in bulk SAC 396 solder alloys by evaluating mechanical behavior may produce correlations to mechanical joint degradation.

Constant strain-rate and constant load compression tests were performed to record time independent (stress-strain) and time dependent (creep) deformation behavior as a function of Au content. “Ring-in-plug” fatigue testing is also currently underway to examine fatigue relationships as a function of Au content. Specific material property values can then be extracted from the collected data and applied to a unified creep constitutive plasticity model (UCPM) which will be discussed in the next paper. This paper addresses the empirical mechanical trends of SAC396 solder as a function of Au levels.

Experimental Procedures

Compression testing methodologies were utilized to generate stress-strain and creep deformation relationships. Detailed explanations of the test setups have been described elsewhere [20, 21]. A servohydraulic load frame was used for both tests. Figure 1 illustrates the test setup. Resistive heating or cold air flow was employed to produce "hot" or "cold" test temperatures, respectively.

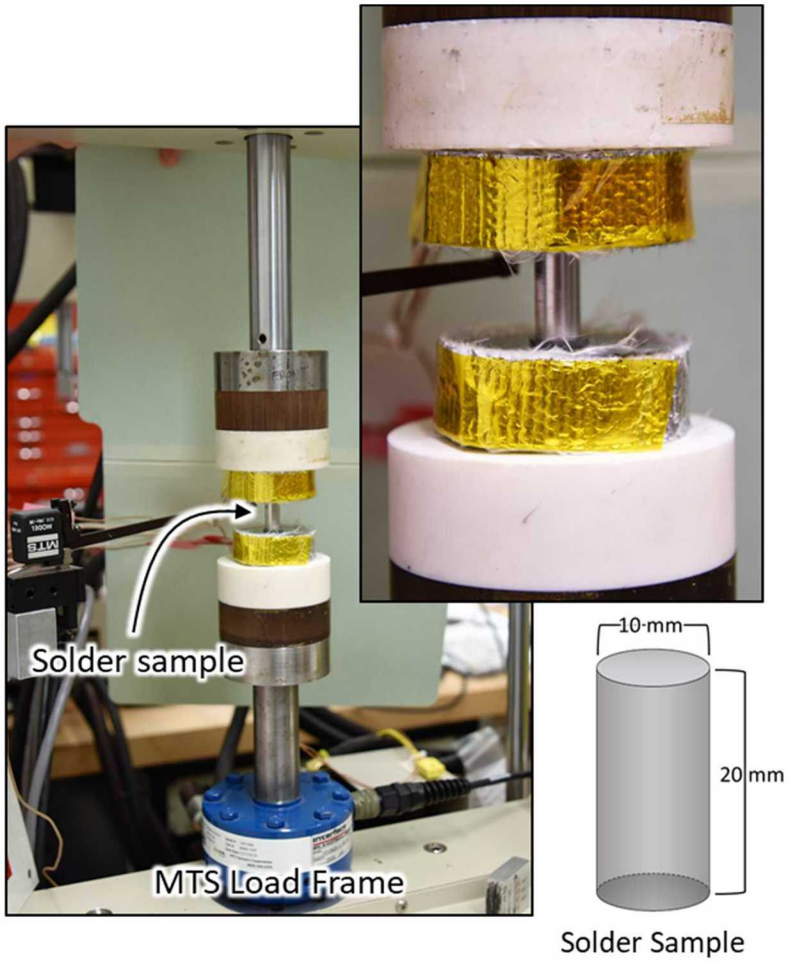

Figure 1. Test frame set-up for stress-strain and creep compression tests and schematic of cylindrical solder sample with nominal dimensions.

The samples used for these tests were alloys cast into cylindrical "bullet" shapes with nominal height and diameter of 20 and 10mm, respectively. SAC 396/Au formulations were melted in house with the appropriate amounts of Au to generate 7 compositions containing 0-8wt.% Au. These compositions are meant to represent compositions that might manifest during and after soldering, as Au from an Au coating dissolves into molten solder or diffuses into solder over time. Figure 2 shows a mold used to produce the cast "bullets."

Figure 2. Bullet mold immediately after molten solder was poured (left) and after rotating the mold top (right).

Compression Stress-Strain Testing

Compression stress-strain testing was performed to examine elastic deformation behavior as a function of Au content in SAC 396. Two pre-specified strain rates were imposed on the sample and the uniaxial displacement was recorded as a function of the stress required to maintain the strain rate. Time is unimportant except to define when the test will be stopped. 7 compositions in 3 aged conditions were tested at 5 temperatures for 2 strain rates.

Aging conditions were performed to generate data that would reflect as-soldered and in-service joint behavior.

Figure 3 illustrates the testing matrix for a given composition. Note that this matrix was applied to all compositions.

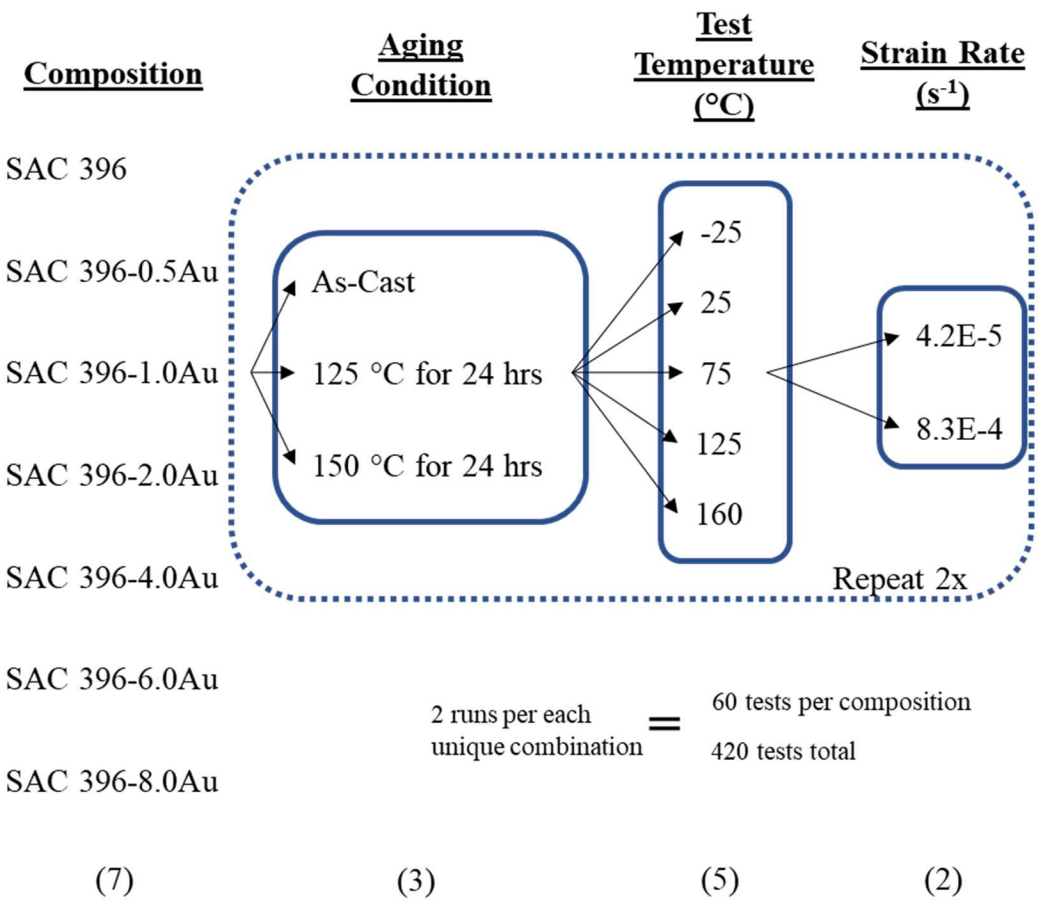

Figure 3. Testing matrix for stress-strain compression testing. Samples for a given composition are subjected to 1 of 3 aging conditions. Compression testing is then performed at 5 different temperatures and 2 different strain-rates.

The recorded load-displacement curves are used to generate true stress-strain curves (from initial engineering stress-strain curves), from which yield stress, yield strain, and static elastic modulus values can be extracted. Figure 4 illustrates how the recorded data is converted into the true stress-strain curves.

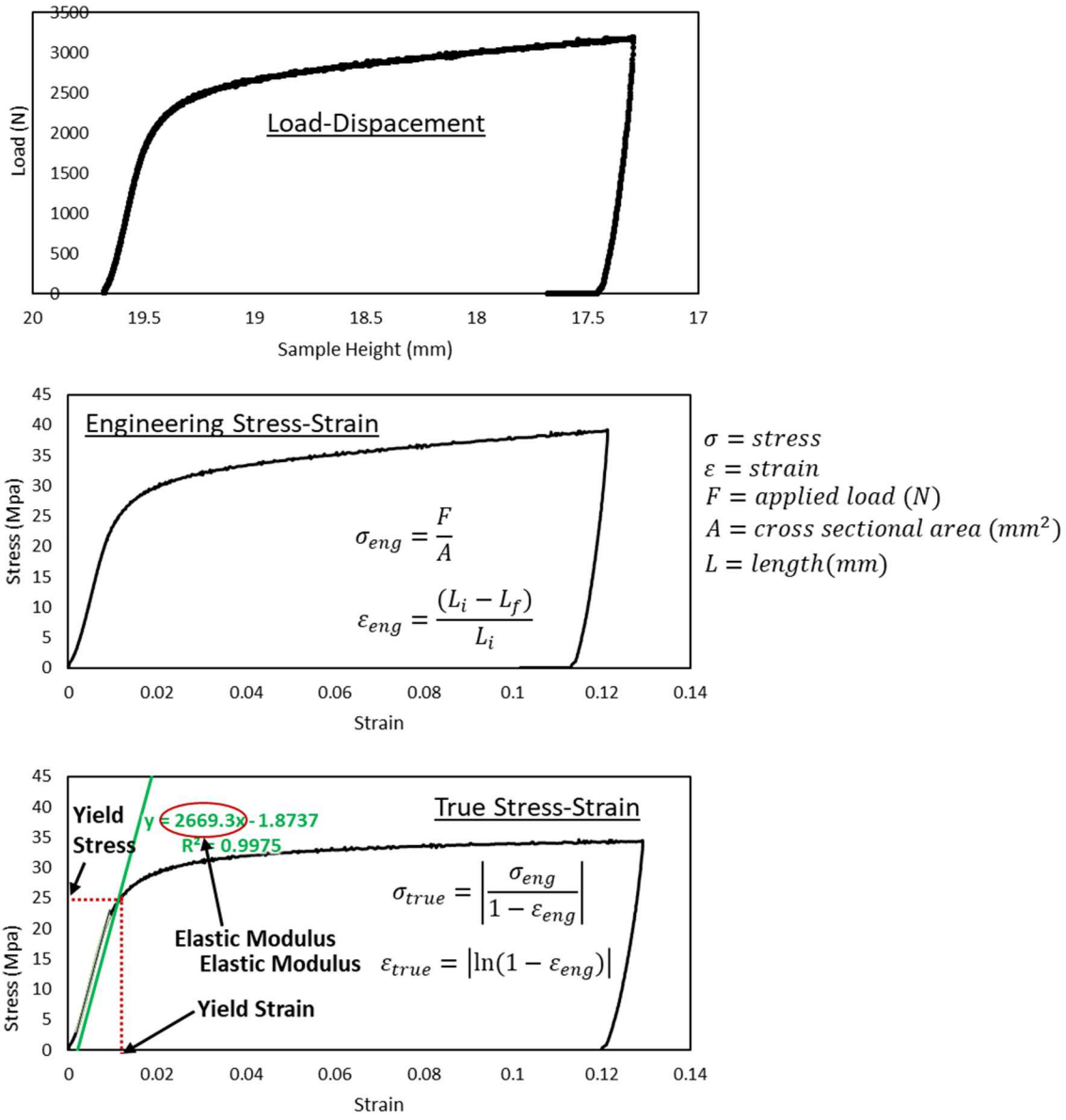

Figure 4. From top to bottom, the progression from the recorded load-displacement data to a true stress-strain curve.

True stress-strain curves were calculated to account for the instantaneous diameter changes during compression.

Compression Creep Testing

Compression creep testing was performed to understand the plastic deformation behavior as a function of Au content. In this test, a constant load (rather than strain-rate) is applied to a bulk solder sample, and displacement vs. time is recorded. The resulting deformation is therefore time dependent. A given test ends after 10% strain is realized or 50 hours, whichever occurs first. The test matrix for the creep

testing is shown in Figure 5. At this point, “as-cast” samples have been tested at 125 and 25 °C. Testing at the other three temperatures continues.

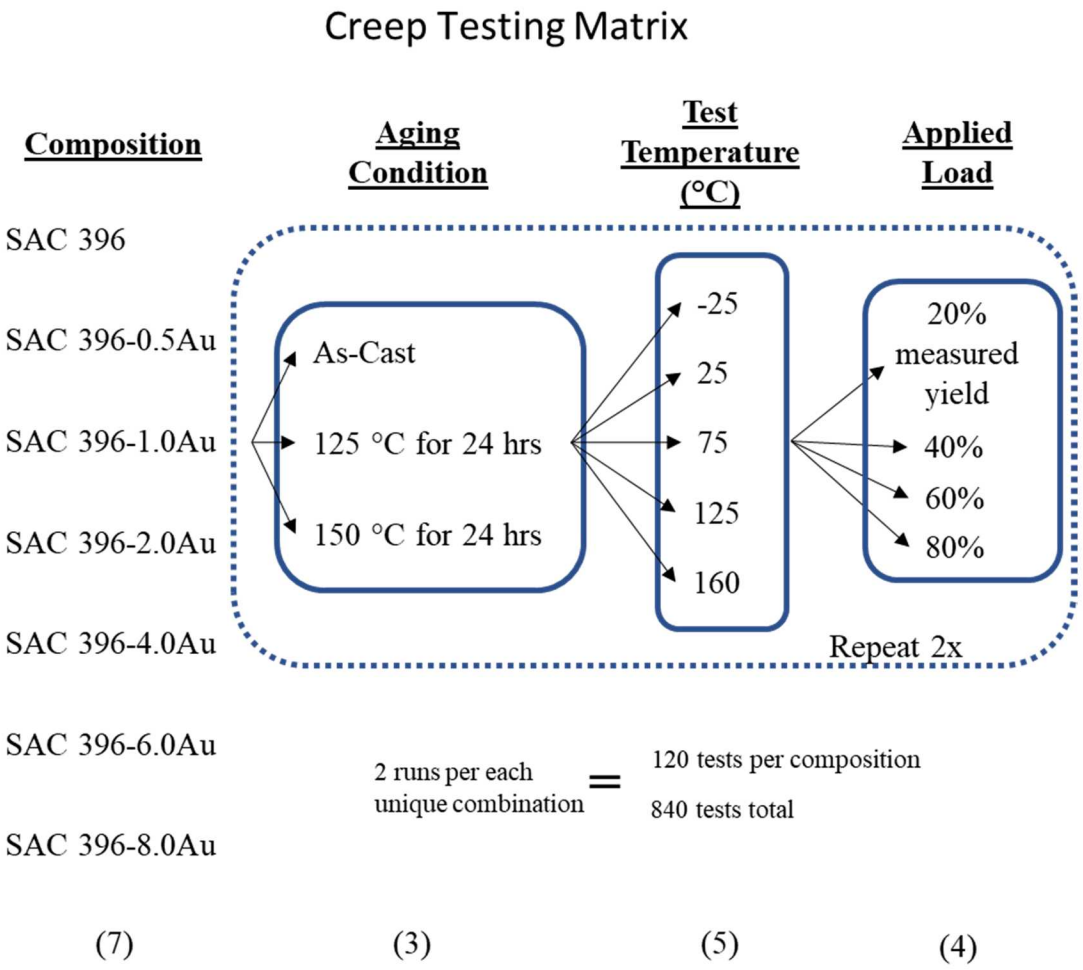

Figure 5. Testing matrix for constant-load, creep compression testing. Samples for a given composition are subjected to 1 of 3 aging conditions. Compression testing is then performed at 5 different temperatures and 4 different loads.

The applied loads are percentages of the measured average yield stress (YS) values from the previous stress-strain testing.

Creep curves are generally separated into three regions, primary, secondary, and tertiary, as shown in Figure 6.

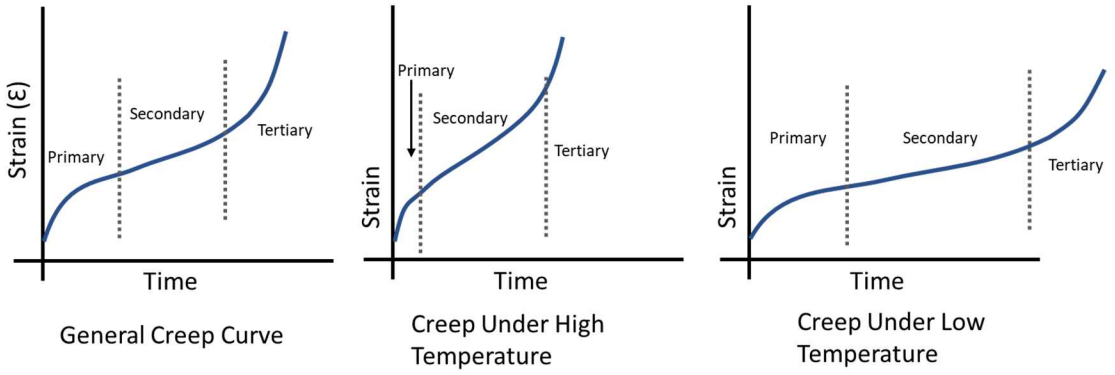

Figure 6. A typical creep curve (left), showing the 3 regions that accompany creep deformation as well as the role that temperature can play regarding time spent in each region.

When a sudden load is realized, a relatively rapid displacement occurs in the *primary* stage. The rate of displacement decreases until a linear, steady-state condition follows in the *secondary* stage. This steady-state creep rate is the lowest creep rate that the material will experience, until finally, a rapid creep rate increase occurs in the *tertiary* stage prior to failure.

The goal of the current creep testing is to measure this minimum, steady-state creep rate from the secondary stage to calculate activation energy and time constants by comparing behavior at various temperatures. Figure 7 illustrates how the recorded data was translated to describe activation energies.

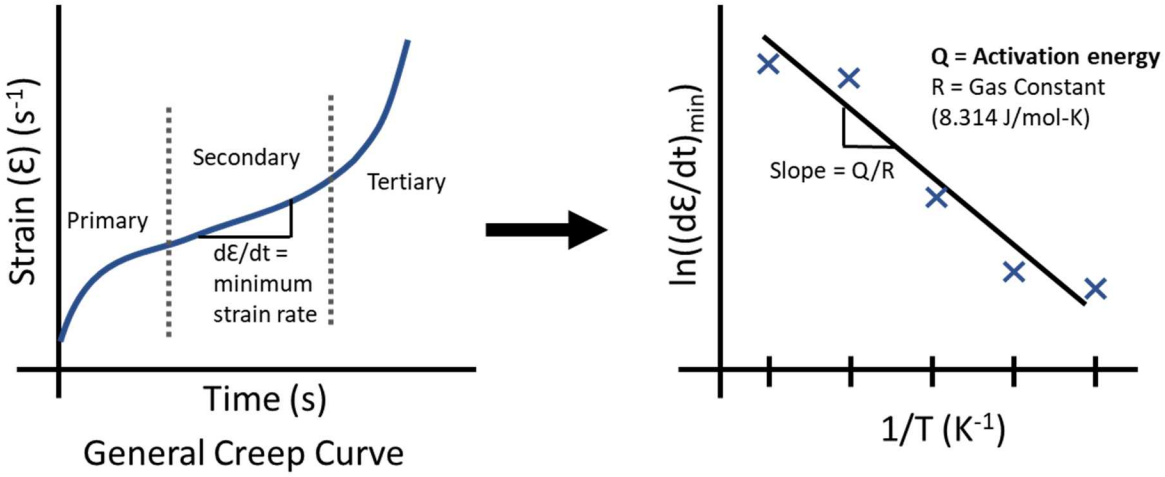

Figure 7. Using the measured displacement over time to determine the secondary stage minimum strain rate (dƐ/dt) (left) to determine the activation energy required to support creep deformation.

"Ring-in-Plug" (RIP) Fatigue Testing

The high-cycle fatigue response of Au-contaminated SAC396 is also currently being evaluated using the "in house" RIP Fatigue test, but results are not yet available. The sample setup is shown in Figure 8. Test temperature, strain ranges, and frequencies are the key variables. Essentially, a thin, Cu ring is soldered into a larger concentric ring. A small, positive and negative vertical load is then applied over an extended period via a test frame. These loading conditions simulate the low load, high cycle conditions a joint may experience in vibrating conditions. SnPb, SAC396, and SAC396/Au solders will be tested, with the intent to apply the data to the development of an HCF solder joint model.

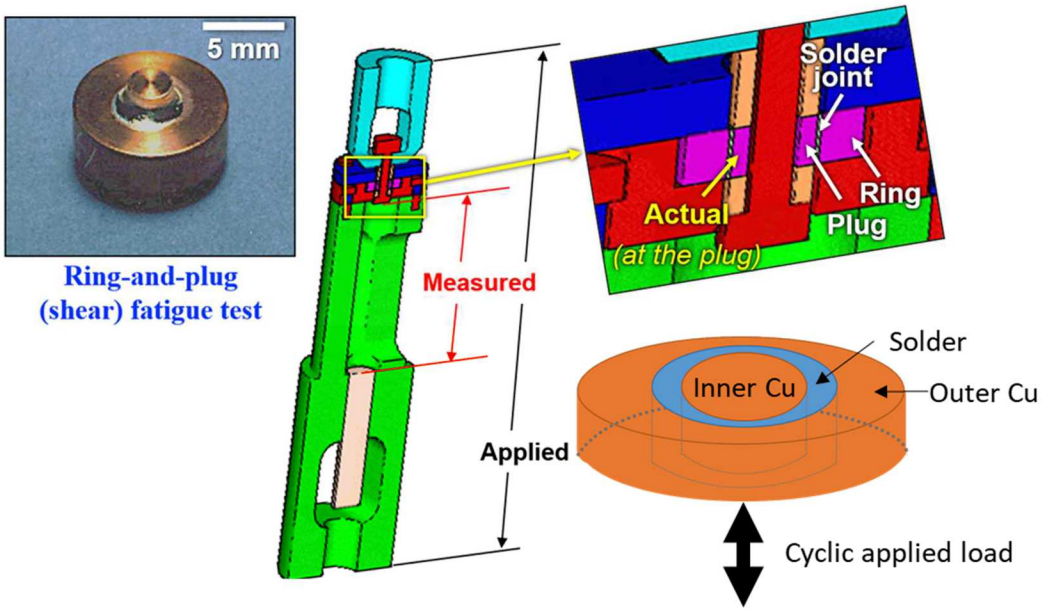

Figure 8. The RIP Fatigue test setup.

Metallography

Untested and tested solder bullets were longitudinally sectioned, and representative optical images were taken near the center for all compositions. SEM/EDS analysis has been performed on 0, 2, 4, and 8 wt.% Au-containing solder. This analysis is preliminary to provide visual distinction between the compositions and aging conditions.

Results/Discussion

Data selected to be reflective of the entire set are presented and discussed below, but Appendix A contains all the data for the stress-strain testing. The creep data to date is discussed, and a comprehensive complementary Appendix is planned for all the creep results.

Compression Stress-Strain Testing (Time independent, stress-strain relationship)

The test temperature, composition, aging condition, and strain-rate effects regarding the experimental yield stress, yield strain, and elastic modulus measurements are presented and discussed below. A significant amount of data was generated in this study, and both the obvious trends and unique exceptions are discussed.

Test Temperature Effect

Test temperature appears to have had the largest effect on yield stress, regardless of composition, aging condition, or strain-rate. Figure 9 illustrates average yield stress measurements for all as-cast compositions for each test temperature and strain-rate. As temperature increases, yield stress decreases for all compositions, though more drastically for those with higher Au levels. The fact that temperature changes produce a similar trend in all 7 alloys highlights the importance of temperature control during

electronic fabrication, storage, and use, regardless of the solder composition.

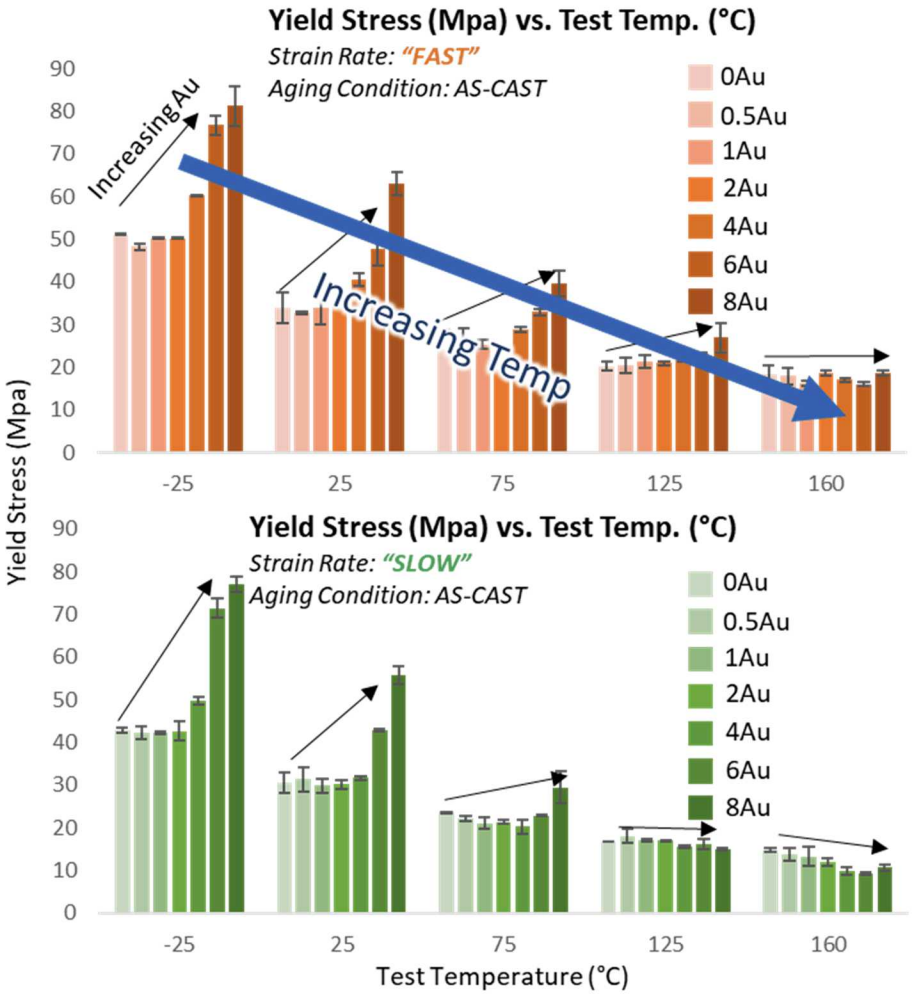

Figure 9. Average (of 4 tests) yield stress values for each of the SAC396/Au "As-Cast" compositions for a given test temperature. The "high" and "low" strain rates are differentiated by the top and bottom plots, respectively.

Yield strain also decreases with increasing temperature, as shown in Figure 10, but the largest apparent changes occurs between -25 and 25 °C, after which the yield strain drop is much more gradual.

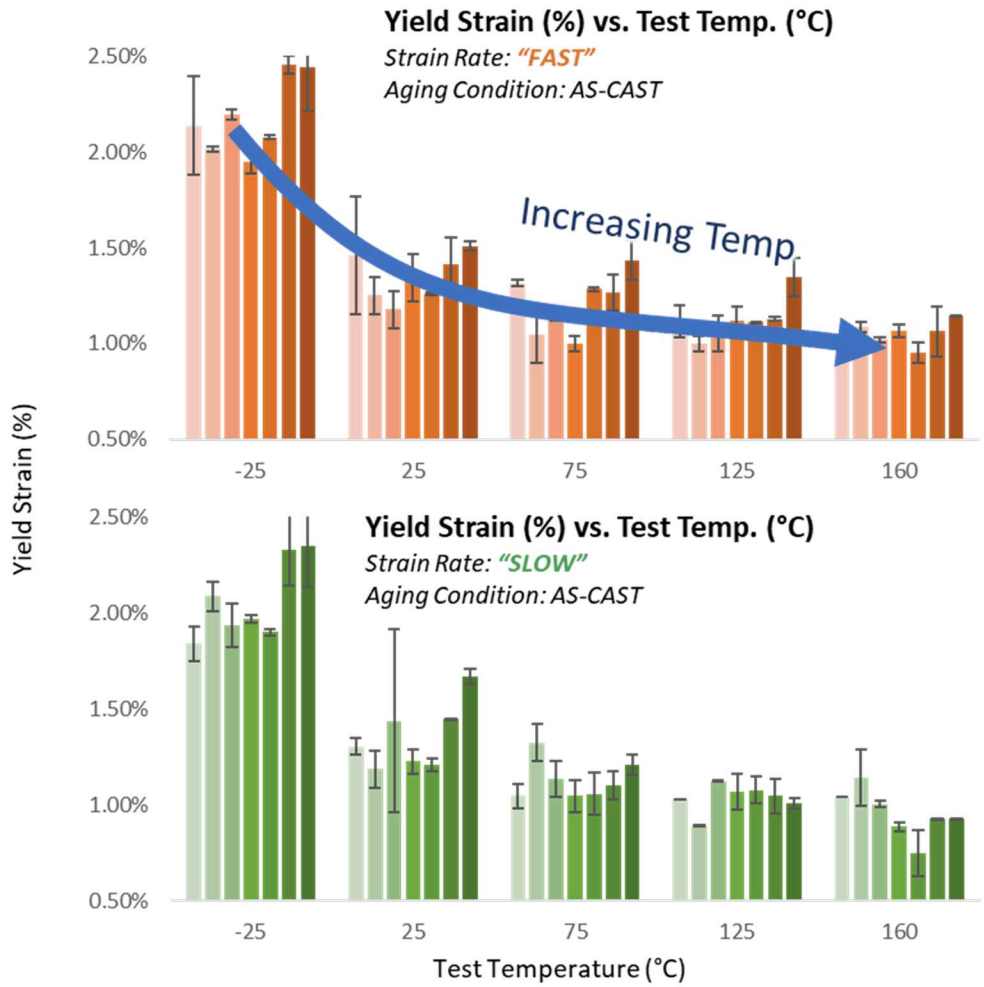

Figure 10. Average (of 4 tests) yield strain values for each of the SAC396/Au "As-Cast" compositions for a given test temperature. The "high" and "low" strain rates are differentiated by the top and bottom plots, respectively.

Inelastic strain occurs sooner with increasing temperature as thermal energy provides a larger driving force for deformation mechanisms.

Modulus trends actually increase initially, before decreasing above room temperature, shown in Figure 11.

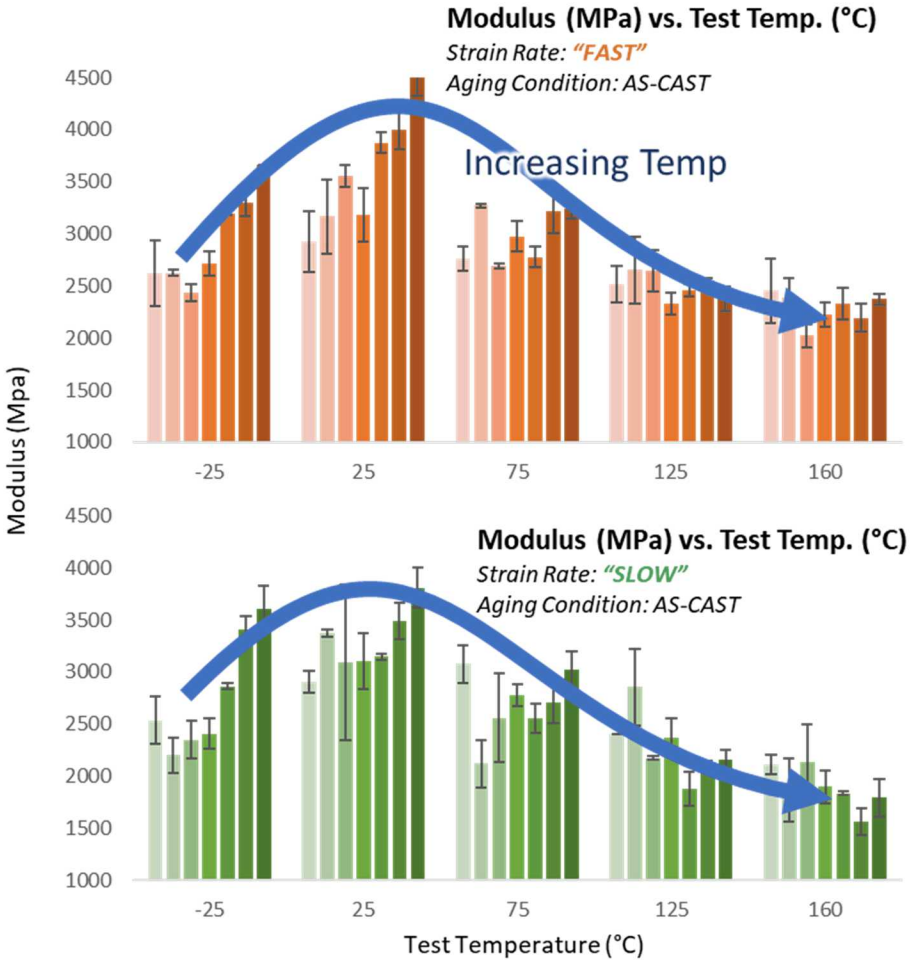

Figure 11. Average (of 4 tests) modulus values for each of the SAC396/Au "As-Cast" compositions for a given test temperature. The "high" and "low" strain rates are differentiated by the top and bottom plots, respectively.

Trends that contain positive and negative slopes are indicative of two competing mechanisms, each dominating over the other in different regimes. In this case, the regimes are test temperatures. At low temperatures it is possible that compositional changes are reflected as metallurgical bonding changes with Au additions. However, at higher temperatures, these metallurgical considerations are overwhelmed by the added thermal energy into the material system.

Composition Effect

As test temperature increases, yield stress decreases, regardless of composition. However, also as temperature increases, the Au content matters less. High Au contents dramatically increase yield stress at -25, 25, and even 75 °C, but at 125 and 160 °C, all compositions behave similarly. The increase in yield stress (and conceivably, strength) is due to the solidification and precipitation of SnAu intermetallics (IMCs), which inhibit the movement of dislocations, and hence require higher stress conditions for yielding to occur. However, as temperature increases, the thermal energy both increases the driving force for deformation mechanisms and may also promote IMC growth. Enough thermal energy may support Au

dissolution throughout the microstructure leading to a degree of composition homogenization. The impact is great enough to overshadow any strength realization due to Au IMC precipitates. It is clear though, that at solder joint service temperatures, Au content has a significant effect on mechanical behavior above 2 wt. % Au contents. It will be imperative to understand how these mechanical properties are reflected in solder joint performance.

Since the relative effects of Au on mechanical performance change with temperature, it will also be important to be aware that when cycling (between hot and cold) solder with more gold, greater property differentials will be realized. Therefore, cycling may have a greater impact on solder joints with relatively higher Au contents.

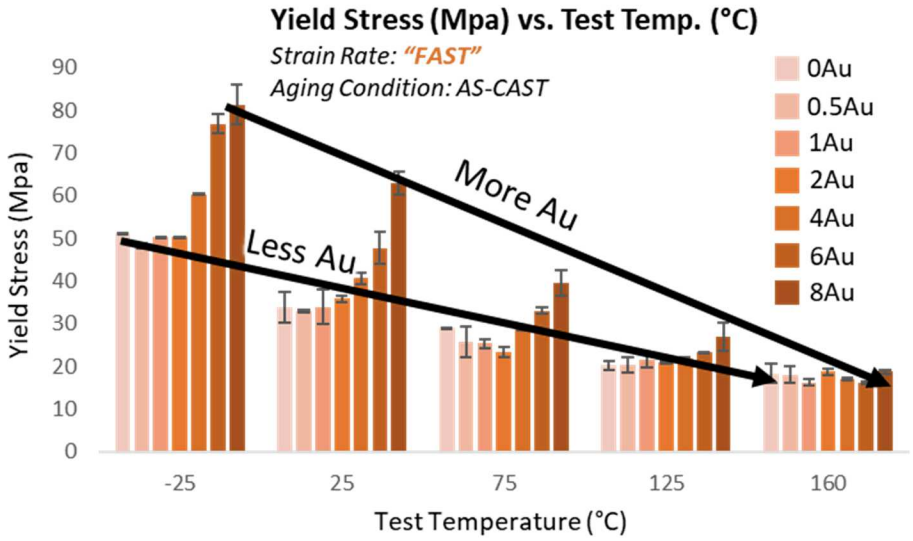

Figure 12. Reiterating yield stress data as a function of Au content and test temperature to illustrate how temperature cycling low Au-containing solder results in less mechanical property change, relative to a high Au-containing solder.

A notable exception regarding the temperature and composition effects is shown in Figure 13. To this point, only the "as cast" aging condition has been discussed. In Figure 13, the samples have been aged prior to stress-strain testing. Unlike the tests described earlier, the composition effect is noticeable at all test temperatures. The 6 wt.% Au composition exhibited higher yield stress values than all other compositions (including 8 wt.% Au) at all test temperatures. This unique behavior suggests that some strengthening metallurgical phenomenon is being supported at 6 wt.% Au when aged accordingly which is generally not supported. Sustaining similar conditions in a solder joint (as a cumulation of next assembly and service conditions) may produce unpredictable joint performance.

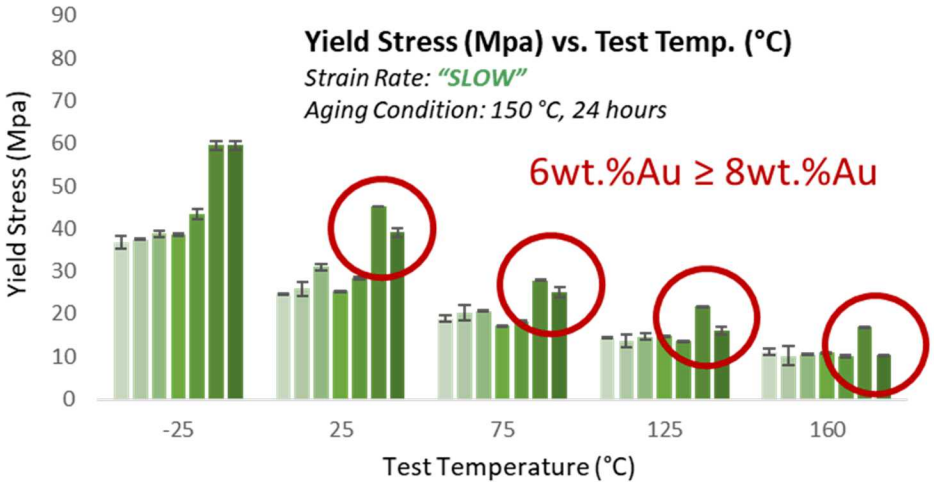

Figure 13. Yield stress as a function of test temperature and composition, reported for the "slow" strain rate for samples that were aged for 24 hours at 150 °C prior to testing.

Aging Effect

In general, aging condition did not result in significant differences in material performance, but the compositions containing higher Au content reflect a greater difference between mechanical behavior after each aging condition compared to the compositions with lower Au content. Higher aging temperatures seem to decrease the composition effect, as shown in Figure 14.

General Trends

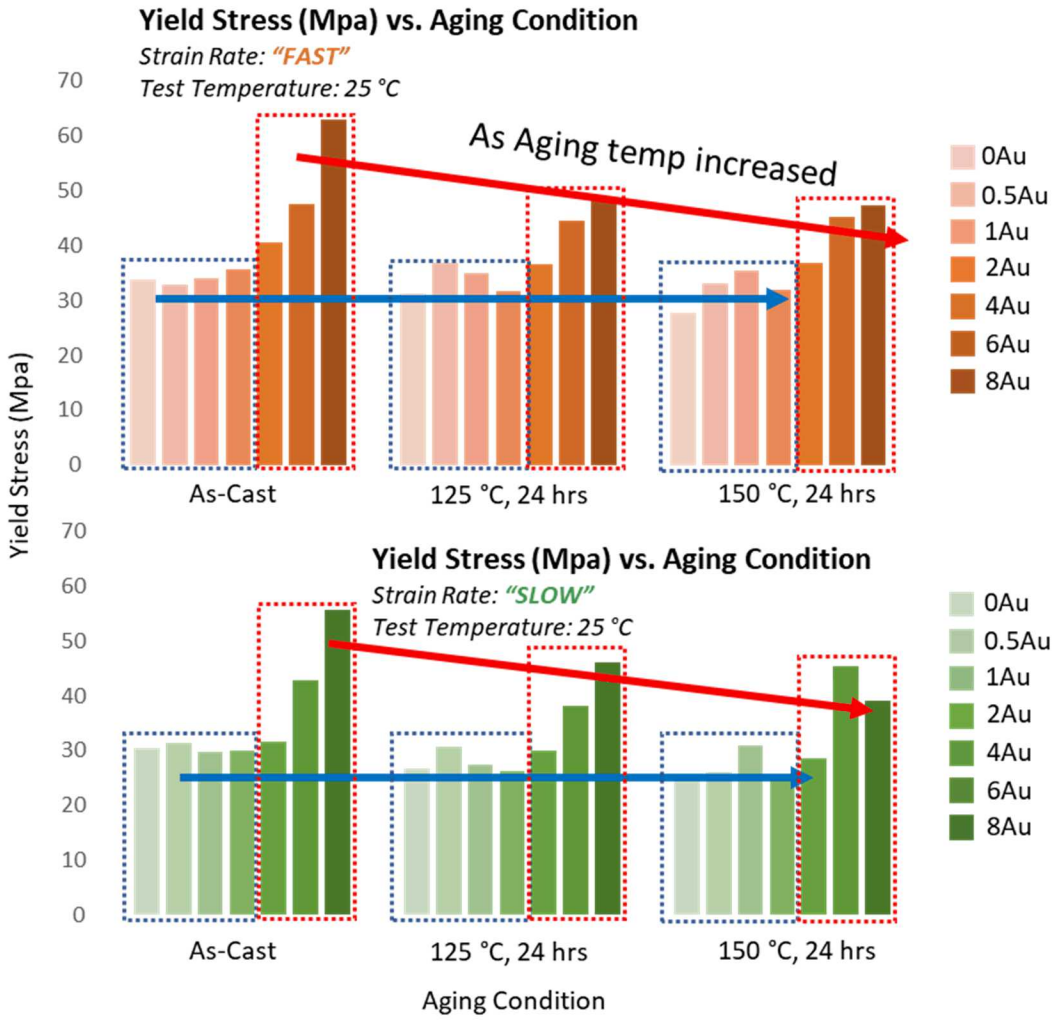

Figure 14. Yield stress values for a given test temperature (25 °C), as a function of composition and aging condition.

Aging at elevated temperatures might promote Au dissolution into the solder matrix, hence producing a more homogenized, stable microstructure. A stable microstructure may support more consistent mechanical performance over a larger range of compositions, therefore understanding the cumulative effect of thermal cycles over a joint's lifetime will be important to understand joint performance in the long-term. Developing optimal heat treatments, post-soldering may also be desired in efforts to stabilize microstructure where potential Au contamination might be suspected.

Strain-Rate Effect

The lower strain rate generally produced lower yield stress, yield strain, and modulus values relative to the higher strain rate. A lower strain rate would have allowed more time for stress induced metallurgical effects to be realized, and therefore promote deformation.

Constant Load Compression Testing (Time dependent, time-strain curves)

Creep testing is currently ongoing, but results to date are discussed. More detail will be available at the time of the conference. Only samples in the "as-cast" aging condition have been tested. Figure 15 and Figure 16 illustrate how the combination of test temperature, applied load, and Au content affect minimum creep rates in SAC396.

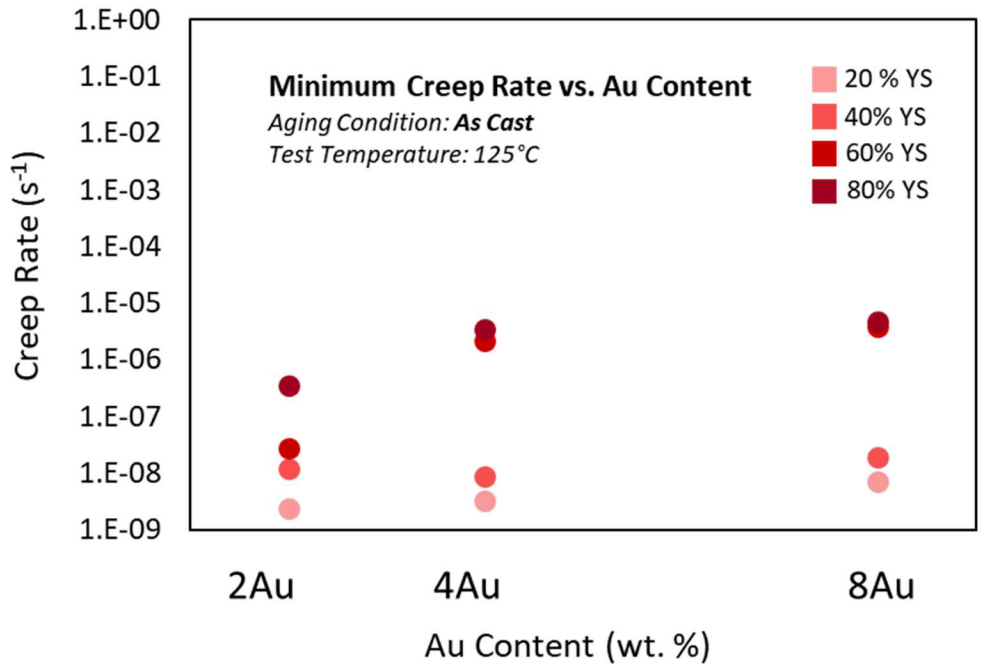

Figure 15. Minimum creep rates for as-cast samples as a function of Au-content in SAC396. The four applied loads were calculated as a percentage of the yield stress values determined from the previous stress-strain testing. The y-axis is plotted on a log scale to show data through 4 orders of magnitude.

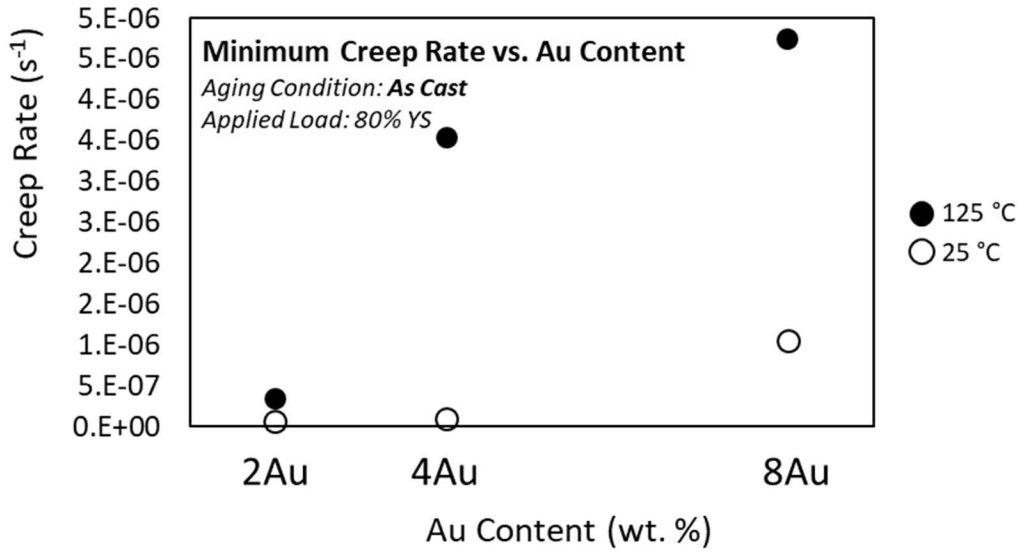

Figure 16. Minimum creep rates for as-cast samples, at one loading condition for two test temperatures, as a function Au-content in SAC396.

Creep results to date are not unusual. Minimum creep rates tend to increase with Au-content, applied load, and test temperature. The higher Au levels seem to magnify the effects of applied load and temperature on the creep rates, also. For example, the 2Au/SAC396 composition exhibited a slight creep rate increase when the test temperature increased from 25 to 125 °C. But the 8Au/SAC396 composition exhibited a much greater creep rate increase when the test temperature also increased from 25 to 125°C.

Thermal cycling which may not have initiated creep processes with low Au-containing solder may pose a more significant problem if the solder contains a lot of Au.

"Ring-in-plug" TMF Testing

Ring-in-plug testing to quantify high cycle fatigue behavior continues, and results may be available at the time of the presentation.

Preliminary Metallography and Microstructure Analysis

Scanning electron microscopy/energy dispersive spectroscopy (SEM/EDS) images of four Au/SAC396 compositions for the three aging conditions are shown in Figure 17, Figure 18, and Figure 19. EDS maps show distributions of Sn, Ag, Cu, and Au.

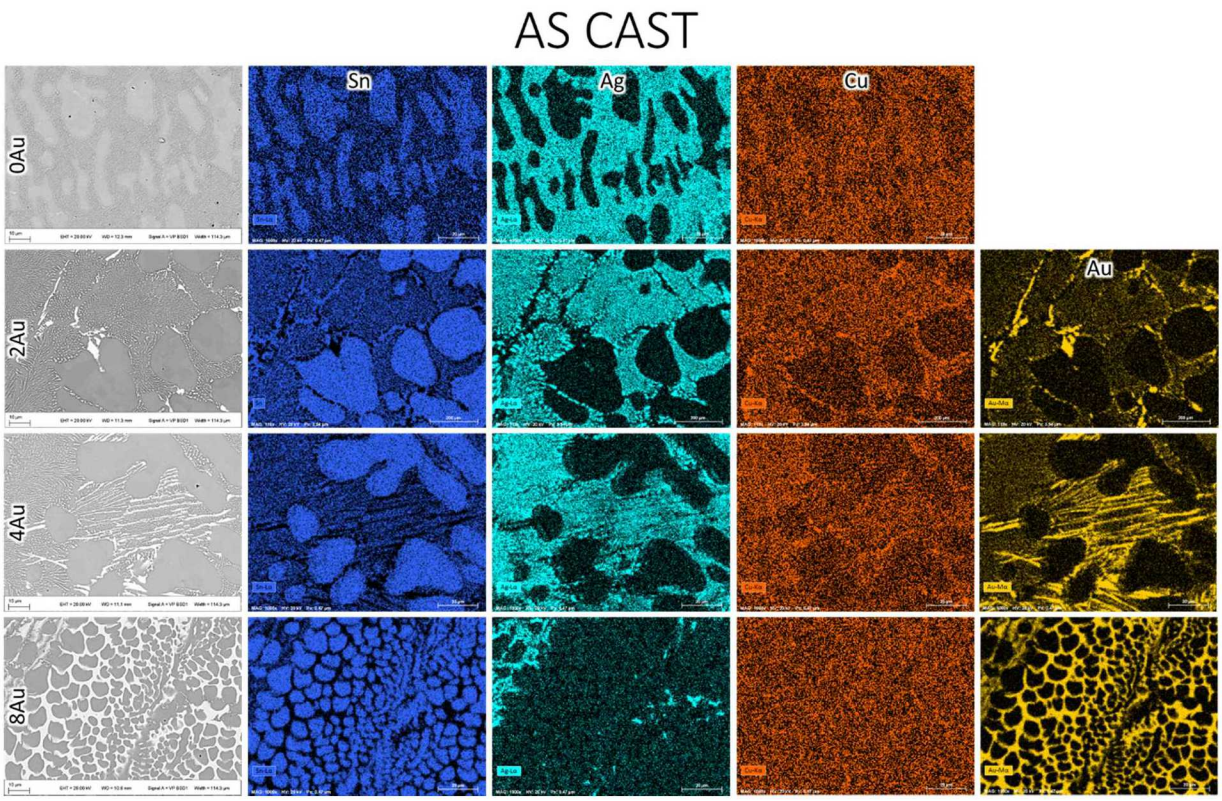

Figure 17. SEM backscatter images and corresponding EDS maps showing Sn, Ag, Cu, and Au elemental distributions for 0, 2, 4, and 8Au/SAC396 bulk samples, in the cast condition.

Qualitatively, the EDS mapping highlights the obvious impact of Au in the SAC 396 microstructure. The top row in Figure 17 shows the pure SAC396 composition without Au. The resulting microstructure is a Sn matrix and a SnAg solid solution with Cu spread throughout both regions. As Au levels increase, Au phases of varying size and morphology increase in concentration.

These microstructures represent those that may form in the bulk solder of a joint. It is important to keep in mind the size and cooling rate differences between the bulk samples cast in this study and that of a solder joint may also impact the as-soldered microstructures. The aging conditions and corresponding microstructures in Figure 18 and Figure 19 attempt to represent bulk solder joint microstructures after next-assembly processing and/or service conditions.

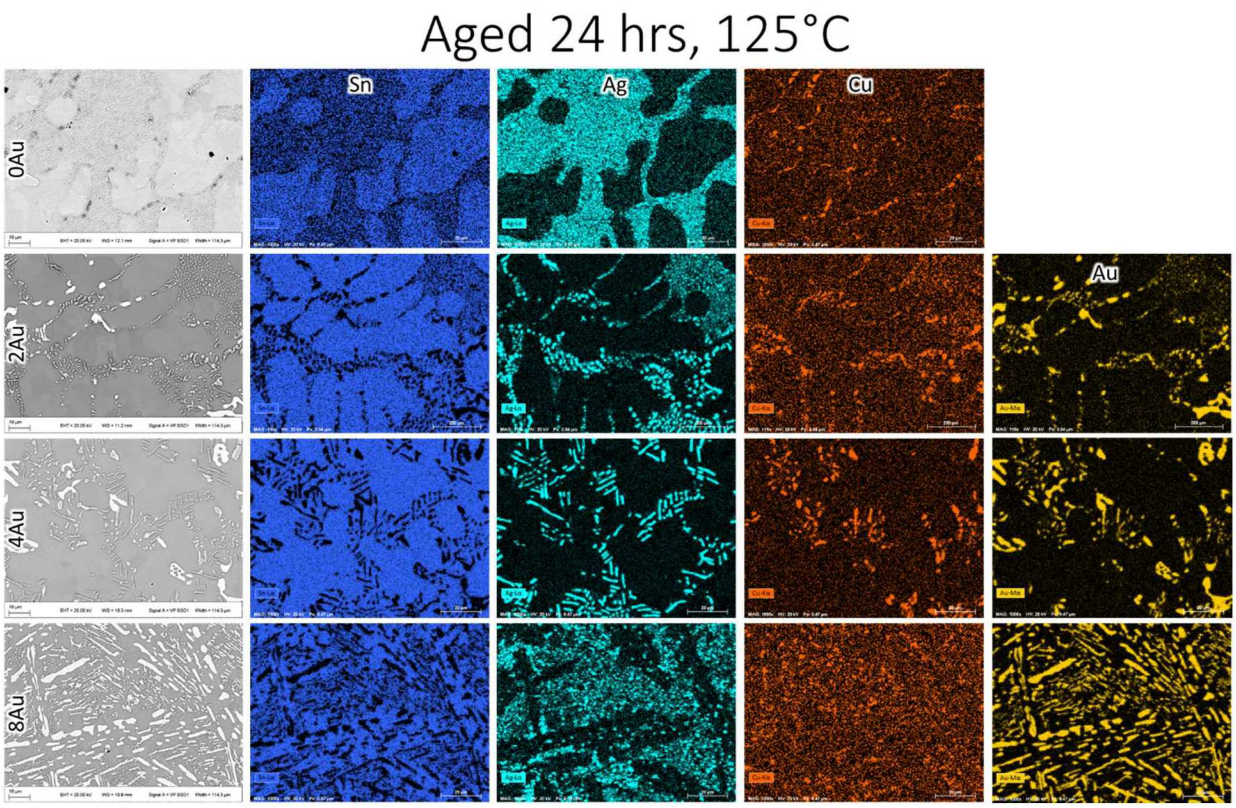

Figure 18. SEM backscatter images and corresponding EDS maps showing Sn, Ag, Cu, and Au elemental distributions for 0, 2, 4, and 8Au/SAC396 bulk samples, aged for 24 hours at 125°C.

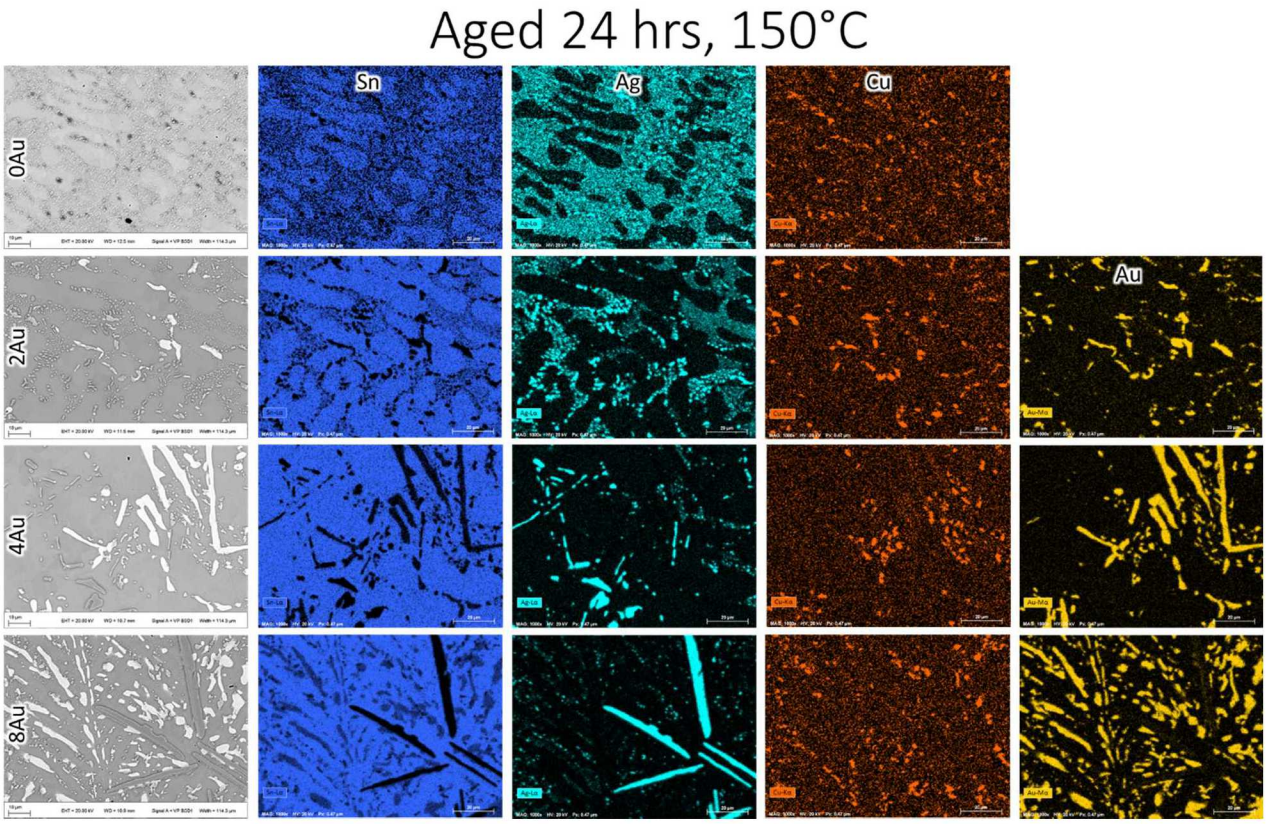

Figure 19. SEM backscatter images and corresponding EDS maps showing Sn, Ag, Cu, and Au elemental distributions for 0, 2, 4, and 8Au/SAC396 bulk samples, aged for 24 hours at 150°C.

Both aging conditions likely promote elemental diffusion which may promote the growth of the as-solidified phases (Figure 17) and formation of new phases. CuAu and AgCuAu regions appear in all heat-treated compositions. Large Ag-rich, needle like phases seem to cluster together in flower-like formations as Au levels increase.

More complete characterization is desired to fully identify phases and microstructural features and will require electron backscatter diffraction (EBSD), transmission electron microscopy (TEM), and differential scanning calorimetry (DSC) methods.

The following three figures compare optical metallographic images of stress-strain tested and untested solder samples.

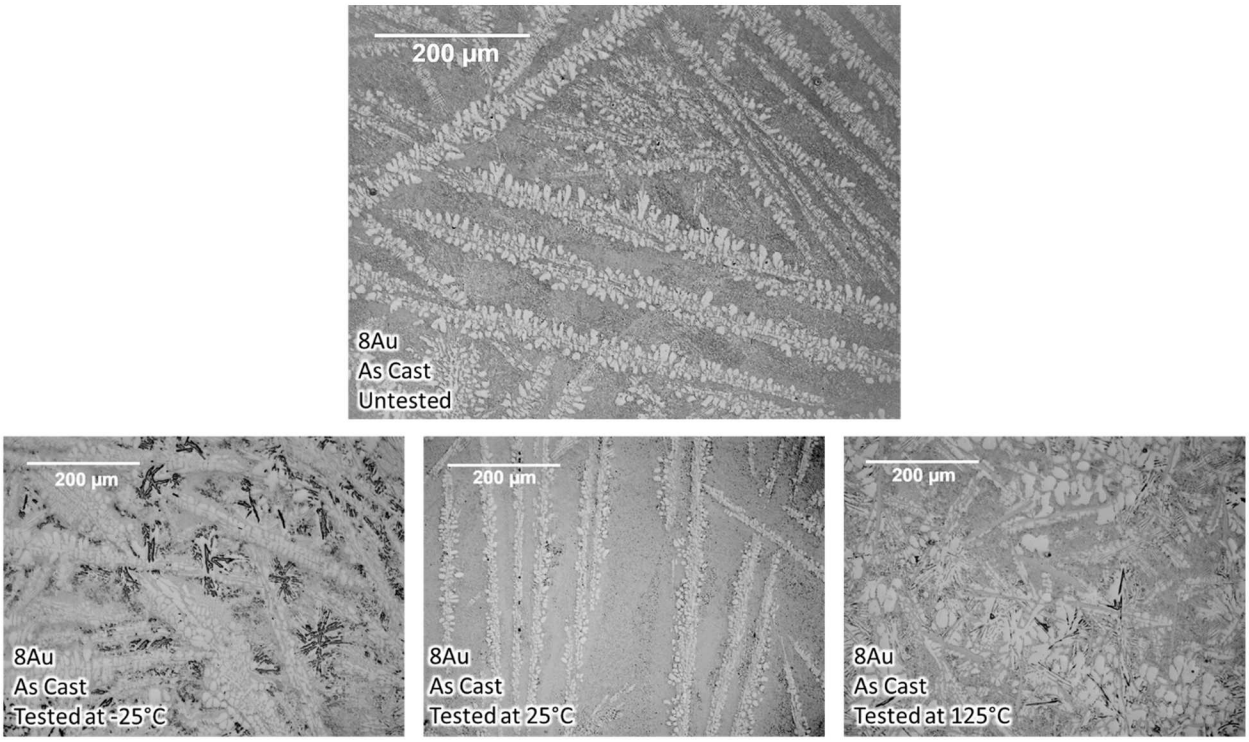

Figure 20. Optical micrographs taken in the center of longitudinal cross-sections of bulk 8Au/SAC396 solder samples. The top image represents an untested sample, and the bottom three images represent as-cast samples tested at -25, 25, and 125 °C (from left to right).

The optical micrographs show no evidence of deformation from the stress-strain tests. It is difficult to relate any deformation behavior with specific phases and/or phase interaction during loading. Stress effects on phase transformations are also possible. Since macroscopic sample deformation was observed, higher resolution characterization methods are likely necessary to observe the metallographic details associated with material deformation.

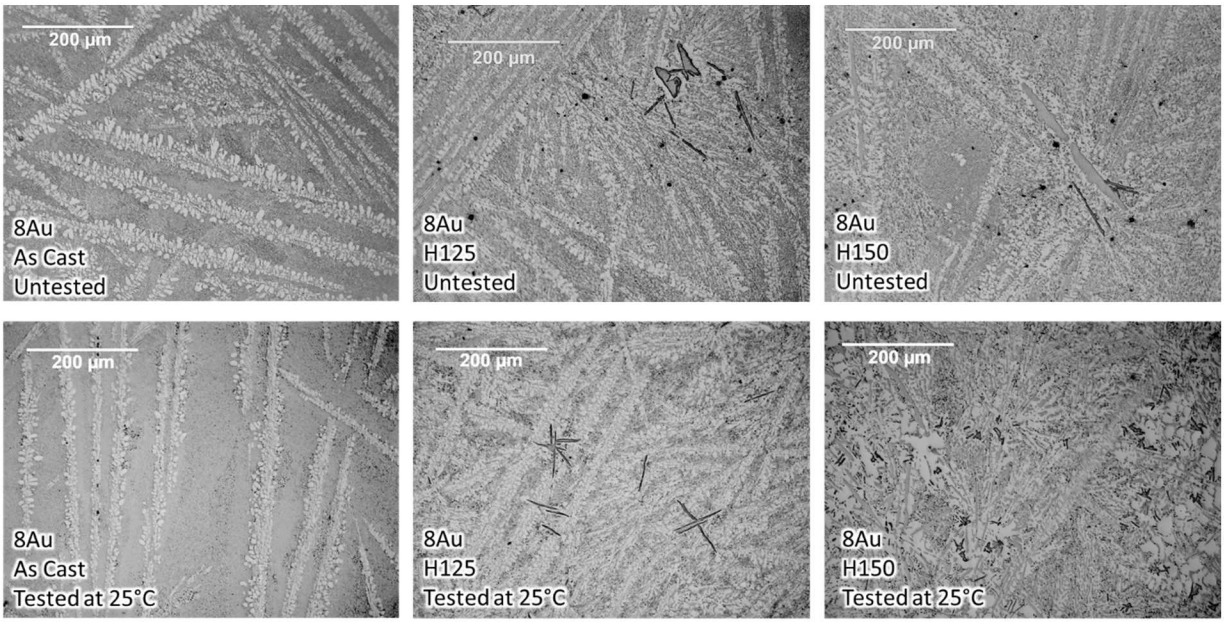

Figure 21. Optical micrographs taken in the center of longitudinal cross-sections of bulk 8Au/SAC396 solder samples. The top images represent an untested sample for each aging condition (as-cast, aged at 125 °C, and aged and 150 °C.) The bottom images represent a stress-strain tested sample for each aging condition.

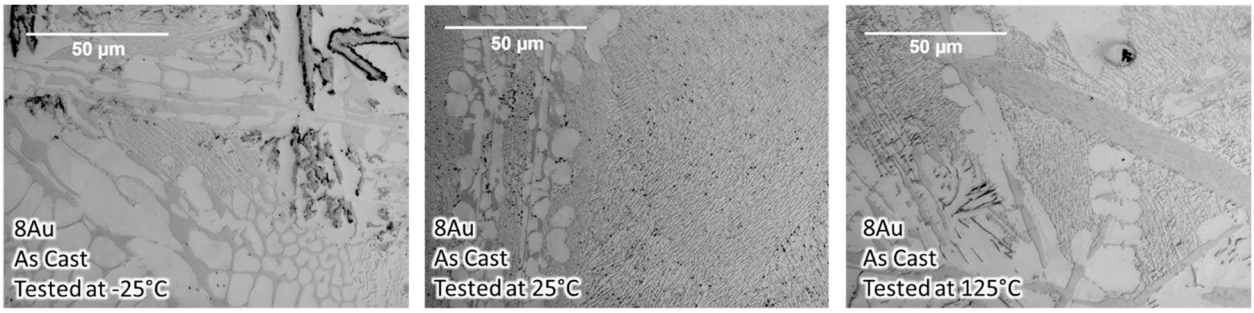

Figure 22. Optical micrographs taken in the center of longitudinal cross-sections of bulk 8Au/SAC396 solder samples. The samples represent the as-cast aging condition but were all stress-strain tested at different temperatures.

Conclusion

Stress-strain compression testing has been completed in order to evaluate the elastic deformation behavior of seven Au/SAC396 compositions. Yield stress decreases with decreasing temperature and increases with increasing Au content. Composition effects are less marked as test temperature increases. Samples that underwent aging reflected less scatter in the data, likely due to microstructure stabilization.

Creep compression testing is in progress to evaluate the plastic deformation behavior of the Au/SAC396 compositions. These compression tests will provide the mechanical properties to expand upon current low cycle fatigue (thermomechanical fatigue) solder modeling capabilities for accounting for Au embrittlement. Minimum creep rates increase with test temperature, Au content, and applied load.

Ring-in-plug fatigue testing is underway to evaluate high cycle fatigue (vibration) behavior of baseline solders and those containing Au. This work supports the development of high cycle fatigue predictive capabilities.

Preliminary metallography has been performed on the seven Au/SAC396 compositions to provide metallurgical explanation for the mechanical behavior. Work continues to provide accurate characterization of bulk tested and untested samples.

More results will be available at the time of the conference.

References

1. Fossum, A.F., et al., *A PRactical Viscoplastic Damage Model for Lead-Free Solder.* Journal of Electronic Packaging, 2006. **128**: p. 71-81.
2. Hare, E., *Gold Embrittlement of Solder Joints*. 2010, SEM Labs, Inc.
3. Foster, F.G., *Embrittlement of Solder by Gold Plated Surfaces*, in *Papers on Soldering: ASTM Special Technical Publicaton*. 1963, ASTM. p. 13-20.
4. Manko, H., *Solders and Soldering*. 4th ed. 2001, New York: McGraw-Hill.
5. Bester, M.H. *Metallurgical Aspects of Soldering Gold and Gold Plating*. in *International Electronics Packaging and Production Conference*. 1968. Brighton, England.
6. Hillman, C., et al., *Gold Embrittlement in Lead-free Solder*. 2014, DFR Solutions: Beltsville, MD.
7. Duckett, R. and M.L. Ackroyd, *Influence of Solder Composition on the Embrittlement of Soft-soldered Joints on Gold Coatings.* Electroplating and Metal Finishing, 1976. **29**(5): p. 13.
8. Zeng, K. and K.N. Tu, *Six Cases of Reliability Study of Pb-free Solder Joints in Electronic Packaging Technology.* Materials Science and Engineering R, 2002. **38**: p. 55-105.
9. Pan, J., et al., *Effect of Gold Content on the Reliability of SnAgCu Solder Joints.* IEEE Transactions on Components, Packaging and Manufacturing Technology, 2011. **1**: p. 1662-69.
10. Syed, A. *Reliability and Au Embrittlement of Lead Free Solders for BGA Applications*. in *International Symposium on Advanced Packaging Materials*. 2001. Georgia, USA: Institute of electrical and Electronics Engineers.
11. Vianco, P.T., *Embrittlement of Surface Mount Solder Joints by Hot Solder-Dipped, Gold-Plated Leads*, in *Surface Mount Technical Association International Conference*. 1993: San Jose, CA
12. Harding, W.B. and H.B. Pressley. *Soldering to Gold Plating*. in *50th Annual Convention: American Electroplaters' Society*. 1963. American Electroplater's Society.
13. Banks, S., *Reflow Soldering to Gold.* Electronic Packaging and Production, 1995. **35**(6): p. 69-74.
14. Glazer, J., P.A. Kramer, and J. J.W. Morris, *Effect of Gold on the Reliability of Fine Pitch Surface Mount Solder Joints.* Circuit World, 1992. **18**(4): p. 41-47.
15. Tegehall, E., *Review of the Impact of Intermetallic Layers on the Brittleness of Tin-Lead and Lead-Free Solder Joints*. 2006, IVF Industrial Research and Development Corporation: Sweeden.
16. Kotadia, H.R., P.D. Howes, and S.H. Mannan, *A Review: On the Development of Low Melting Temperature Pb-Free Solders.* Microelectronics Reliability, 2014. **54**: p. 1253-1273.
17. Huang, K., et al., *Study of Interfacial Reactions Between Sn(CU) Solders and Ni-Co Alloy Layers.* Journal of Electronic Materials, 2010. **39**: p. 2403-2411.
18. Wolverton, M. *Solder Joint Embrittlement Mechanisms, Solutions, and Standards*. in *IPC APEX EXPO*. 2014. Las Vegas, USA: Association Connecting Electronics Industries.
19. Park, J.-Y., et al., *Influence of Au Addition on the Phase Equilibria of Near-Eutectic Sn-3.8Ag-0.7Cu Pb-Free Solder Alloy.* Journal of Electronic Materials, 2003. **32**(12): p. 1474-1482.
20. Vianco, P., J. Regent, and A. Kilgo, *Time-Independent Mechanical and Physical Properties of the Ternary 95.5Sn-3.9Ag-0.6 Cu Solder.* Journal of Electronic Materials, 2003. **32**: p. 142.

21. Vianco, P. and J. Regent, *The Compression Stress-Strain Behavior of Sn-Ag-Cu Solder.* J. Met., 2003. **55**: p. 50.

Appendix A: Compression Stress-Strain Results for all Test Temperatures, Compositions, Aging Conditions, and Strain Rates

The first three sections illustrate the yield stress, yield strain, and modulus as a function of test temperature. The last three sections show **THE SAME DATA** portrayed as a function of aging condition.

Yield Stress (MPa) vs. Test Temperature (°C)

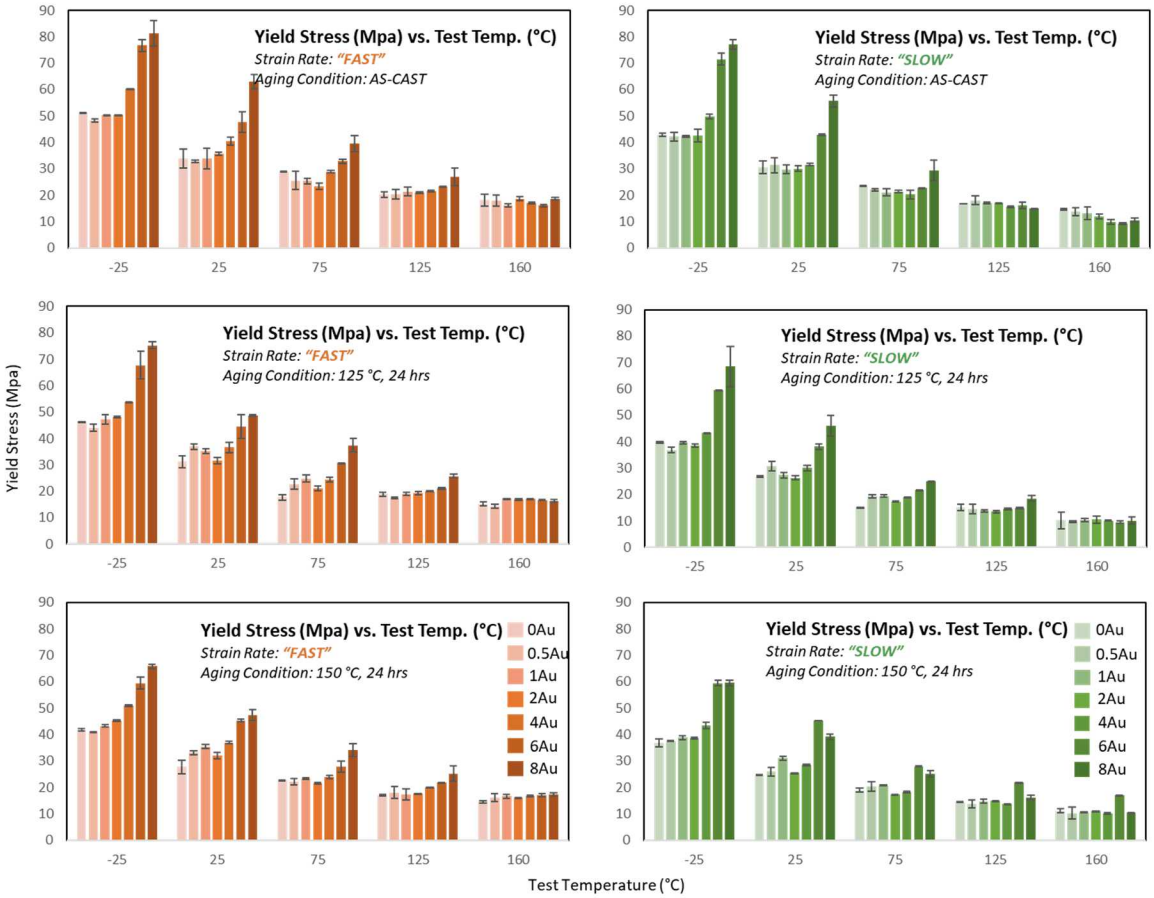

Yield Strain (%) vs. Test Temperature (°C)

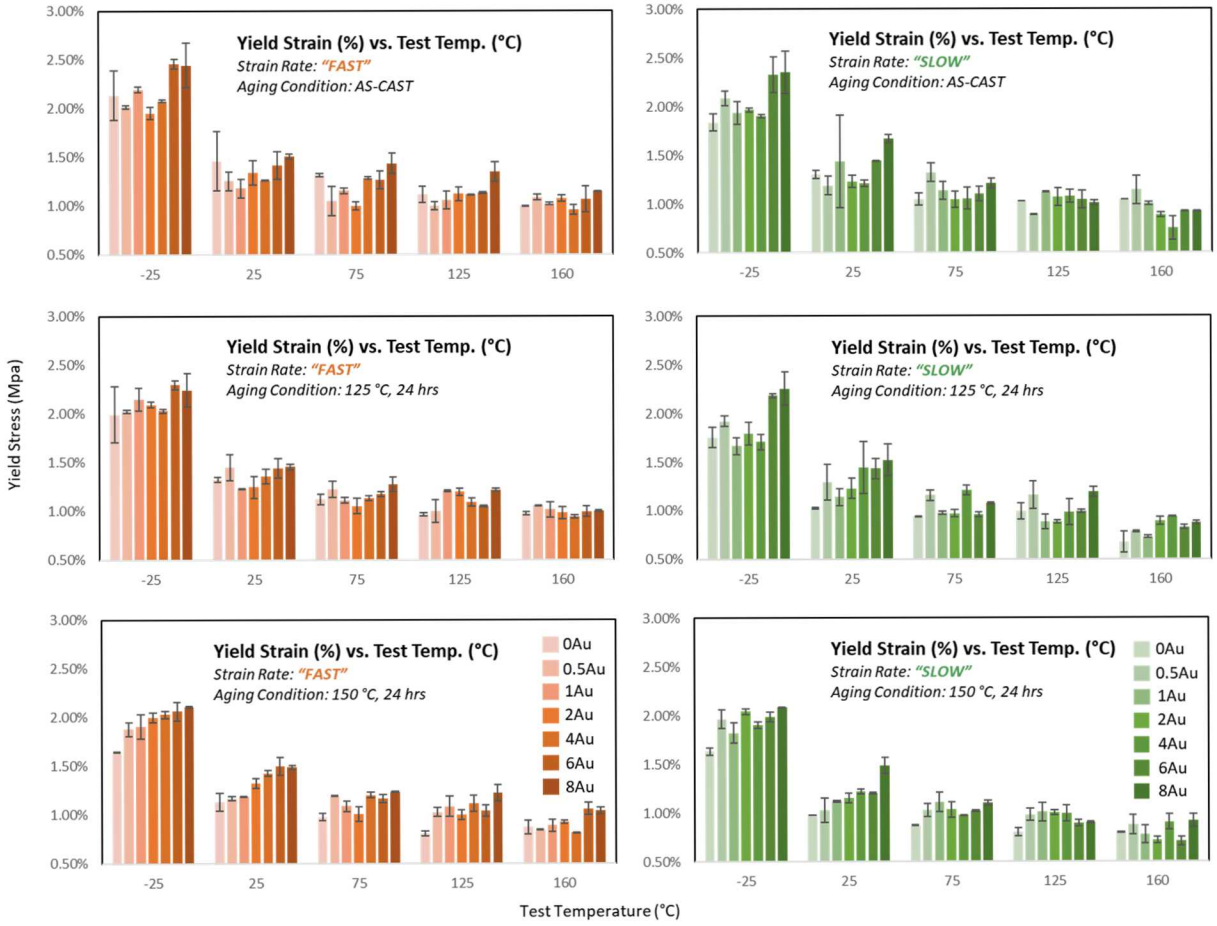

Modulus (MPa) vs. Test Temperature (°C)

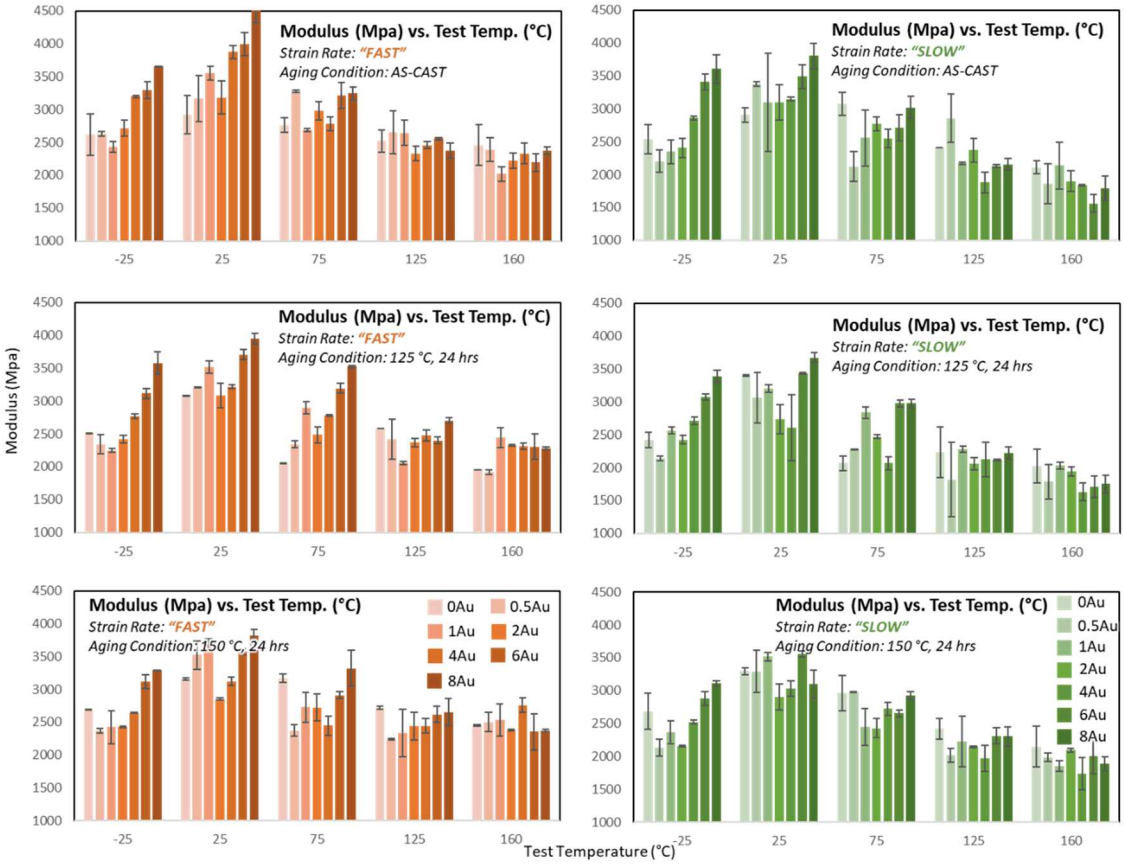

Yield Stress (MPa) vs. Aging Condition

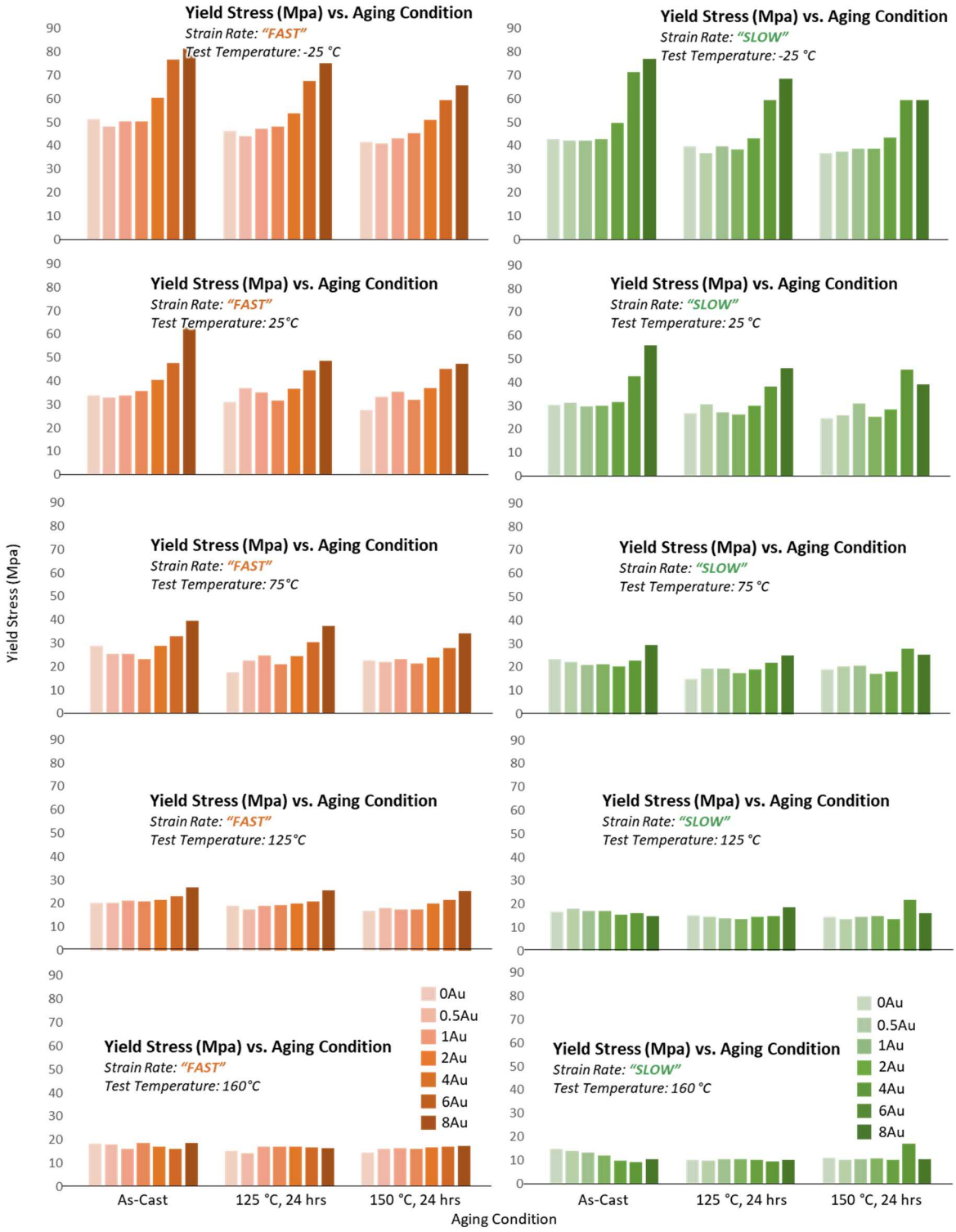

Yield Strain (%) vs. Aging Condition

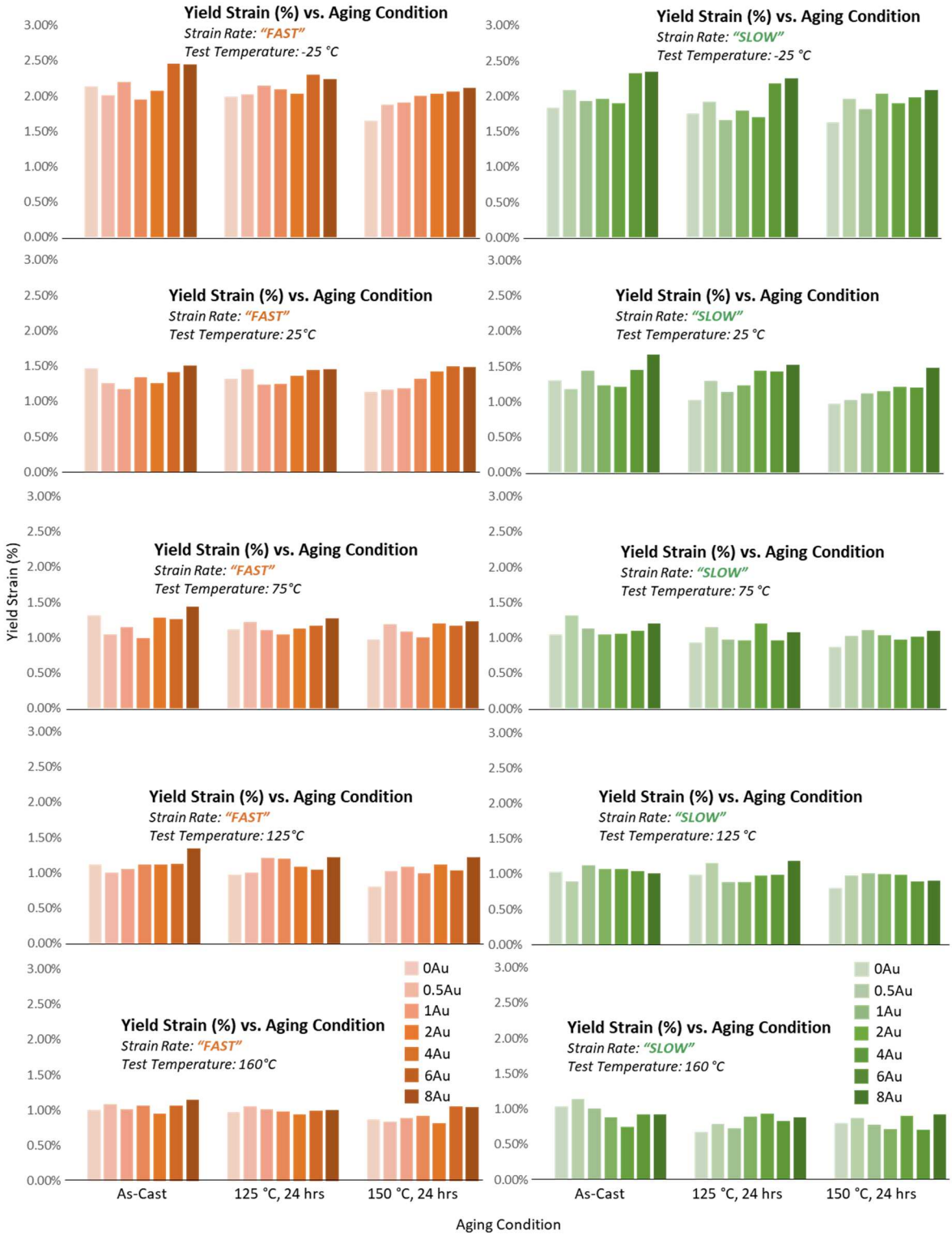

Modulus (MPa) vs. Aging Condition